Physics Letters B 803 (2020) 135306

Contents lists available at ScienceDirect

Physics Letters B

www.elsevier.com/locate/physletb

GW170817 constraints analyzed with Gogny forces and momentum-dependent interactions

O. Lourenço [a,*], M. Bhuyan [b,c], C.H. Lenzi [a], M. Dutra [a], C. Gonzalez-Boquera [d], M. Centelles [d], X. Viñas [d]

[a] Departamento de Física, Instituto Tecnológico de Aeronáutica, DCTA, 12228-900, São José dos Campos, SP, Brazil
[b] Department of Physics, Faculty of Science, University of Malaya, Kuala Lumpur 50603, Malaysia
[c] Institute of Research Development, Duy Tan University, Da Nang 550000, Vietnam
[d] Departament de Física Quàntica i Astrofísica and Institut de Ciències del Cosmos (ICCUB), Facultat de Física, Universitat de Barcelona, Martí i Franquès 1, E-08028 Barcelona, Spain

ARTICLE INFO

Article history:
Received 27 June 2019
Received in revised form 13 February 2020
Accepted 13 February 2020
Available online 17 February 2020
Editor: J.-P. Blaizot

Keywords:
Equation of state
Finite-range interactions
Neutron star
Tidal deformability
Moment of inertia

ABSTRACT

A set of equations of state obtained from finite-range Gogny forces and momentum-dependent interactions is used to investigate the recent observation of gravitational waves from the binary neutron star merger GW170817 event. For this set of interactions, we have calculated the neutron star tidal deformabilities (related to the second Love number), the mass-radius diagram, and the moment of inertia (I). The I-Love relation has been verified. We also have found strong correlations among the tidal deformability of the canonical neutron star, its radius, and the derivatives of the nuclear symmetry energy at the saturation density. Most of the obtained results are located within the constraints of the tidal deformabilities extracted from the GW170817 detection.

1. Introduction

The theoretical analysis of astronomical observations of very dense matter in the Universe has disclosed that various properties of neutron stars (NSs), such as the mass-radius relation, the moment of inertia, and the tidal deformability, are very sensitive to the properties of nuclear matter at saturation and also at supra-nuclear densities. Hence, it is important to study theoretically the core of NSs, which in the center can attain densities of several times ρ_0, where ρ_0 is the saturation density. Different nuclear models have since long been applied to analyze the properties of matter at these supra-nuclear densities through the equation of state (EoS), see e.g. [1–5] and references therein. The recent LIGO and Virgo observation of GW170817 [6–8], accounting for a merger of two NSs, has enhanced the present interest to examine the sensitivity of the EoS at large values of density and isospin asymmetry. Furthermore, the extracted NS tidal deformabilities of the binary system with 90% and 50% confidence limits, see Fig. 1 of Ref. [7], have provided a new constraint for the nuclear EoS. Many EoSs have been studied under β-equilibrium to formulate various connections between the tidal deformability (related to the second Love number) and other quantities [9–14] as, for instance, the moment of inertia (I). This specific correlation is named as I-Love relation, and it seems to be universal, i.e., EoS-model independent.

The total mass is one of the best established observables of NSs from many observational studies. Among them, there are the recent accurate observations of highly massive NSs, corresponding to $(1.928 \pm 0.017)M_\odot$ [15,16] and $(2.01 \pm 0.04)M_\odot$ [17] for the PSR J1614-2230 and PSR J0348+0432 pulsars, respectively, with $M_\odot$ being the solar mass. As a result, a great effort has been addressed to derive nuclear models able to generate EoSs that predict such massive objects (see [18,19] and references therein). However, a precise mass measurement is not enough to completely constrain the underlying EoS. One would also need a precise measurement of the radius of the NS whose mass has been obtained. The uncertainties in the determination of the NS radius are still an open question for observational studies [20–22]. The Neutron Star Interior Composition Explorer (NICER) mission is already set up with the aim to provide a measurement of the radius with accuracy of order 5%. Moreover, the recent GW170817 observation of a NS merger [6–8] has dramatically changed the present status of the nuclear matter models by adding new constraints.

* Corresponding author.
E-mail addresses: odilon.ita@gmail.com (O. Lourenço), bunuphy@yahoo.com (M. Bhuyan).

https://doi.org/10.1016/j.physletb.2020.135306

For several decades, a large amount of theoretical studies have been performed using different models to describe strongly interacting cold matter at high baryon densities in NSs [22–25]. Very recently, many hadronic matter models have been tested and tried to constrain their outcomes with the observed tidal boost in the gravitational wave (GW) detection from the binary NS merger GW170817 [6–8]. Among these studies, nonrelativistic models [9,26–29], effective field theories [30,31], and the relativistic mean-field description of nucleons interacting via meson exchange [9,14,24], have significantly contributed to correlate nuclear observables at saturation density with the cold nuclear matter at very high densities. On the other hand, studies based on effective quark models are focused on the existence of a possible quark matter phase and on the role of color superconductivity at high densities [18,32–36]. Other recent studies relating the tidal deformability to dense matter properties can also be found, for instance, in Refs. [37–40]. Our aim in this work is to try to understand the behavior of NS matter at high densities using finite-range interactions of Gogny type [41,42] and of momentum-dependent interaction (MDI) type [43,44], which are very successful in nuclear physics as we point out below. Our investigations will focus on the examination of the applicability of the presented interactions in describing the recent data on the GW170817 event [7], on the search for possible correlations between matter bulk parameters and the tidal deformability, and on the verification of the I-Love relation.

The paper is organized as follows. Sec. 2 gives a brief description for the Gogny and MDI interactions applied to stellar matter. The results of our calculations are presented in Sec. 3. Sec. 4 includes a short summary and the concluding remarks.

2. Gogny forces and MDI interactions for stellar matter

The Gogny forces were introduced by D. Gogny in order to describe the mean field and the pairing field within the same interaction. They consist of a density-dependent zero-range term and two finite-range Gaussian terms that generate the momentum dependence of the Gogny potential. Gogny forces are well adapted for describing the ground-state systematics as well as deformation and excitation properties of finite nuclei. An exhaustive compilation of nuclear properties computed with the D1S Gogny force [45] can be found in [46]. New Gogny forces such as D1N [47] and the highly accurate D1M [48] have been proposed. D1N and D1M take into account the microscopic neutron matter EoS of Friedman and Pandharipande [49] in the fit of their parameters and improve on the description of isovector properties. It has been found, however, that when one applies the usual parametrizations of the D1 family to studies of NSs, they can not reach masses of $\sim 2M_\odot$. To remedy this situation, a reparametrization of the D1M force called D1M*, which predicts maximum masses of $2M_\odot$ when the associated EoS is used to solve the Tolman-Oppenheimer-Volkoff (TOV) equations, has been formulated very recently [42]. The Gogny parametrizations chosen to be analyzed here are those studied in Ref. [42], namely, the D1M, D1M* and D2 forces. D2 [50] is another recent Gogny interaction where the density-dependent contact term has been replaced by a finite-range term, and which also delivers NS masses of $2M_\odot$. Besides, we include in the study the D1M** force [51], which is fitted similarly to D1M* but it is required to predict a NS maximum mass of $1.91M_\odot$, corresponding to the lowest bound of the astronomical observations.

The MDI interactions [43] have been extensively used to study heavy-ion collisions [43,52]. Similar to the Gogny case, the MDI force may be expressed as a zero-range contribution plus a finite-range term, but with a Yukawa form factor instead of a Gaussian. A parameter x of the MDI interaction can be varied to modify the uncertain density dependence of the symmetry energy and of the neutron matter EoS, without changing the EoS of symmetric nuclear matter and the symmetry energy at the saturation density. The MDI model with the tuned isospin dependence has also been used to describe hot asymmetric matter [52] and the properties of NSs [44] and most recently it has been applied to study the tidal deformability of NSs [53]. In our study, we select MDI parametrizations with $-1 \leqslant x \leqslant 0.2$. This leads to a symmetry energy slope L_0 at the saturation density (namely, $L_0 = 3\rho_0\, \partial E_{\rm sym}(\rho)/\partial\rho|_{\rho_0}$) in the range of 51 MeV $\leqslant L_0 \leqslant$ 106 MeV for the MDI forces, whereas the range predicted by the Gogny parametrizations used here is 25 MeV $\leqslant L_0 \leqslant$ 45 MeV (see Table 1 below). One can verify that these two boundaries for L_0 are compatible with those found in Ref. [54] ($L_0 = 58.9 \pm 16.5$ MeV) and used in Ref. [55], in Ref. [56] (40.5 MeV $\leqslant L_0 \leqslant$ 61.9 MeV), in Ref. [18] ($L_0 = 58.7 \pm 28.1$ MeV), and in Ref. [57] ($L_0 = 60 \pm 15$ MeV). We note, however, that some of the considered MDI forces have a slope parameter L_0 above the upper boundary suggested in these references.

In stellar matter under charge neutrality and β-equilibrium, the weak process and its inverse reaction, namely, $n \to p + e^- + \bar{\nu}_e$ and $p + e^- \to n + \nu_e$, take place simultaneously. At densities for which the electron chemical potential μ_e exceeds the muon mass (m_μ), i.e., $\mu_e > m_\mu$, the appearance of muons in the system is energetically favorable. By considering only these two types of leptons in the NS matter, since we assume that neutrinos can escape due to their extremely small cross-sections, one can write the total energy density and pressure of the system as $\epsilon = \epsilon_{had} + \sum_l \epsilon_l$ and $p = p_{had} + \sum_l p_l$, respectively, where the indexes had and l stand for the hadrons and leptons. In this work the hadronic quantities are calculated using the aforementioned Gogny and MDI interactions, taking into account the following conditions: $\mu_n - \mu_p = \mu_e = \mu_\mu$ and $\rho_p - \rho_e = \rho_\mu$, where $\rho_p = y_p \rho$, and $\rho_l = [(\mu_l^2 - m_l^2)^{3/2}]/(3\pi^2)$ for $l = e, \mu$ (we use the physical values for the electron mass m_e and the muon mass m_μ). The chemical potentials and densities of protons, neutrons, electrons and muons are given, respectively, by μ_p, μ_n, μ_e, μ_μ, and ρ_p, ρ_n, ρ_e, ρ_μ, whereas y_p denotes the proton fraction of the system. In this work we are dealing with NSs old enough to assume that neutrinos have left the star and therefore the β-equilibrium is established between the nucleons, electrons, and muons.

In order to describe a spherically symmetric NS of mass M, we solve the TOV equations [58,59] given (in units of $G = c = 1$) by $dp(r)/dr = -[\epsilon(r) + p(r)][m(r) + 4\pi r^3 p(r)]/r^2 f(r)$ and $dm(r)/dr = 4\pi r^2 \epsilon(r)$, where $f(r) = 1 - 2m(r)/r$. The solution is constrained to $p(0) = p_c$ (central pressure) and $m(0) = 0$. At the star surface, one has $p(R) = 0$ and $m(R) \equiv M$, with R defining the NS radius. To describe the EoS of the matter in the NS core we use the Gogny and MDI interactions. For the NS crust we consider two regions, the outer and the inner crust. For the former, we use the EoS proposed by Baym, Pethick and Sutherland (BPS) [60] in a density region of $6.3 \times 10^{-12}\,{\rm fm}^{-3} \leqslant \rho_{\rm outer} \leqslant 2.5 \times 10^{-4}\,{\rm fm}^{-3}$. Currently, microscopic calculations of the EOS of the inner crust for the different Gogny and MDI interactions are not available. Here, following previous literature [41,42,44,61–63], we use for the inner crust a polytropic EoS of the form $p(\epsilon) = A + B\epsilon^{4/3}$. The index 4/3 assumes that the pressure at these densities is dominated by the relativistic degenerate electrons. For each interaction, we match this polytropic formula continuously to the BPS EoS at the interface between the outer and the inner crust and to the EoS of the homogeneous core at the core-crust transition pressure and energy density computed with the thermodynamical method [41,44,64,65]. Thus, the core-crust matching occurs at the transition point that is predicted by each nuclear model. A similar procedure of description of the stellar matter EoS was performed in Ref. [39]. In this work, the authors analyzed more than 200 Skyrme parametrizations in the light of GW170817, also applying a relativistic Fermi gas EoS for the inner crust as in our case. Another approach used to describe stellar mat-

ter is the unified treatment such as the one developed in Ref. [66] in which possible thermodynamical inconsistencies are avoided. In our calculations, with the present models and with some models where the unified EoS is available, we verified by using different crust prescriptions that the crustal EoS has no significant influence on the results for the tidal deformability Λ. The same conclusion has been brought into notice recently [63].

3. Application to the GW170817 constraints

In a binary NS system, tidal forces originated from the gravitational field induce tidal deformabilities in each companion star analogously to the tides generated on Earth due to the Moon. Deformations in the stars related to the quadrupole moment generate GW in which the phase evolution depends on the tidal deformability [67–69]. In a recent work [6], the LIGO/Virgo Collaboration (LVC) published an analysis on the first detection of GW coming from a binary NS inspiral (the energy flux out of the binary due to the GW emission causes the inspiral motion). The measured data allowed the LVC to determine constraints on the dimensionless tidal deformabilities Λ_1 and Λ_2 for each NS in the binary system, as well as on that one related to a canonical star of $1.4M_\odot$ ($\Lambda_{1.4}$). Later on, in Refs. [7,8], the constraints on the $\Lambda_1 \times \Lambda_2$ region and in the $\Lambda_{1.4}$ value were updated. Here we test the Gogny and MDI interactions against the LVC constraints. In order to do that, we calculate the dimensionless tidal deformability as $\Lambda = 2k_2/(3C^5)$, with the NS compactness given by $C = M/R$ and the second Love number written as

$$
\begin{aligned}
k_2 = {} & \frac{8C^5}{5}(1-2C)^2[2+2C(y_R-1)-y_R] \\
& \times \Big\{2C[6-3y_R+3C(5y_R-8)] \\
& + 4C^3[13-11y_R+C(3y_R-2)+2C^2(1+y_R)] \\
& + 3(1-2C)^2[2-y_R+2C(y_R-1)]\ln(1-2C)\Big\}^{-1}, \qquad (1)
\end{aligned}
$$

with $y_R \equiv y(R)$, where $y(r)$ is obtained through the solution of $r(dy/dr) + y^2 + yF(r) + r^2Q(r) = 0$, that has to be solved as part of a coupled system containing the TOV equations. The quantities $F(r)$ and $Q(r)$ are defined as

$$
F(r) = \frac{1-4\pi r^2[\epsilon(r)-p(r)]}{f(r)}, \qquad (2)
$$

$$
\begin{aligned}
Q(r) = {} & \frac{4\pi}{f(r)}\left[5\epsilon(r)+9p(r)+\frac{\epsilon(r)+p(r)}{v_s^2(r)}-\frac{6}{4\pi r^2}\right] \\
& - 4\left[\frac{m(r)+4\pi r^3 p(r)}{r^2 f(r)}\right]^2, \qquad (3)
\end{aligned}
$$

where $v_s^2(r) = \partial p(r)/\partial\varepsilon(r)$ is the squared sound velocity. See for instance Refs. [67,70–73] for the derivations.

We show in Fig. 1 the NS mass-radius diagrams for the Gogny and MDI parametrizations used in this work. Some quantities related to the maximum NS mass and a canonical NS are shown in Table 1. Concerning the Gogny model, the parametrization D1M* [42] is compatible with the bands coming from constraints derived from data obtained, with some underlying assumptions for the used EoS, by Steiner [74] and Nättilä [21]. It also predicts NSs with $M \sim 2M_\odot$, in agreement with the well-known data from the PSR J1614-2230 [15] and PSR J0348+0432 [17] pulsars. These features for D1M* also hold for the D2 force [50]. Concerning the MDI models, we see that the model with $x = 0.2$ does not reach $1.9M_\odot$, whereas $M_{\max}$ of the other models is above $1.9M_\odot$. A very recent value for the observed largest NS mass of $2.14^{+0.20}_{-0.18}M_\odot$ at

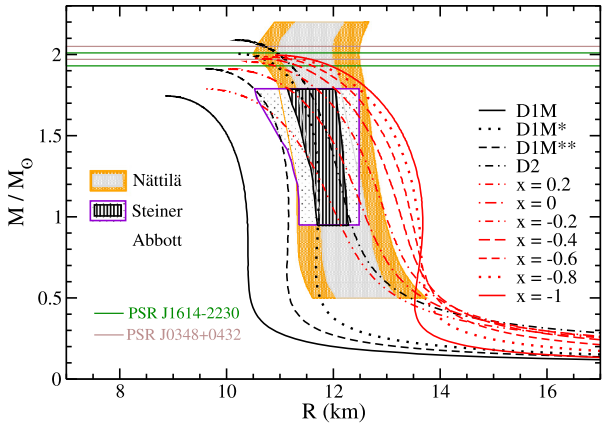

Fig. 1. Neutron star mass-radius diagrams for Gogny and MDI parametrizations. Horizontal bands indicate the masses of PSR J1614-2230 [15] and PSR J0348+0432 [17] pulsars. Outer orange and inner gray bands: constraints extracted from Ref. [21]. Outer white and inner black bands: constraints extracted from Ref. [74].

Table 1
Stellar matter properties obtained from the Gogny and MDI models used here: maximum neutron star mass ($M_{\max}$) with its corresponding radius ($R_{\max}$) and central energy density (ϵ_c), along with the radius ($R_{1.4}$) of a canonical neutron star of mass of $M = 1.4M_\odot$, and its dimensionless tidal deformability ($\Lambda_{1.4}$). The value of the slope parameter L_0 of the symmetry energy for the considered models is shown in the last column.

Model	$M_{\max}$ ($M_\odot$)	$R_{\max}$ (km)	ε_c (fm^{-4})	$R_{1.4}$ (km)	$\Lambda_{1.4}$	L_0 (MeV)
D1M	1.74	8.85	10.40	10.15	122	24.83
D1M*	2.00	10.20	7.74	11.69	316	43.18
D1M**	1.91	9.60	8.78	11.07	221	33.91
D2	2.09	10.16	7.80	11.98	300	44.83
MDI ($x = 0.2$)	1.79	9.58	9.33	11.46	217	51.05
MDI ($x = 0.0$)	1.91	10.00	8.49	12.10	314	60.17
MDI ($x = -0.2$)	1.96	10.32	7.97	12.52	402	69.28
MDI ($x = -0.4$)	1.98	10.54	7.65	12.84	487	78.40
MDI ($x = -0.6$)	1.99	10.70	7.44	13.09	573	87.51
MDI ($x = -0.8$)	1.99	10.82	7.27	13.29	661	96.63
MDI ($x = -1.0$)	2.00	10.91	7.15	13.45	754	105.75

95.4% credible level and of $2.14^{+0.10}_{-0.09}M_\odot$ at 68.3% credible level is proposed in Ref. [75] from the MSP J0740+6620 pulsar. D1M*, D2 and the MDI models with $x \leq -0.2$ would be compatible with the lower limit of this mass at the 95.4% level and only D2 in the case of the 68.3% level.

Still, regarding the values shown in Table 1, we remark that it seems there is at least a trend of a certain "threshold value" of $L_0 \sim 40$ MeV, the lower limit of the range proposed in Ref. [56], below which there are only configurations predicting $M_{\max} < 2M_\odot$ for the maximum NS mass. For instance, this is true for the D1M and D1M** parametrizations and for the 42 parametrizations of Skyrme and relativistic models analyzed in Ref. [76]. A more systematic study in that direction is needed in order to confirm this result for a larger set of models. For now on, we restrict our study only to parametrizations presenting $M_{\max} \sim 2M_\odot$, i.e., we exclude the EoSs of D1M and MDI($x = 0.2$), which predict maximum masses clearly below the observations of Refs. [15–17].

In Fig. 2a we plot the dimensionless tidal deformability Λ as a function of the NS mass. We see that all parametrizations, except the MDI ones with $x = -0.8$ and $x = -1$, reproduce the data from LIGO/Virgo [7] of $\Lambda_{1.4} = 190^{+390}_{-120}$ for the canonical star. Furthermore, by using the results presented in Fig. 2a and in Table 1, it is possible to extract the following fitting expression for $\Lambda_{1.4}$ as a function of the canonical star radius, $\Lambda_{1.4} = aR^b_{1.4}$, with $a = 6.97 \times 10^{-5}$ and $b = 6.19$. Although Λ is defined as proportional to k_2R^5, k_2 is obtained through the solution of the differential equation for y as a function of R, see Eq. (1). This is the

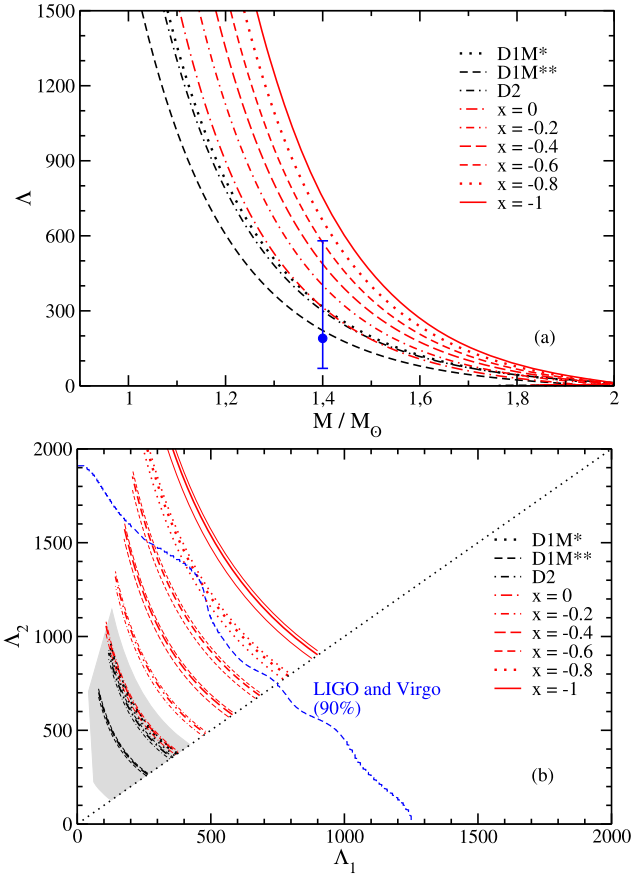

Fig. 2. (a) Dimensionless tidal deformability Λ as a function of the neutron star mass, and (b) dimensionless tidal parameters Λ_1 and Λ_2 related to the high and low mass components inferred from the binary system of the GW170817 event, along with the contour line of 90% credible level (dashed blue curve). The internal and external curves of each parametrization are related to the error in the chirp mass, $\mathcal{M} = 1.188^{+0.004}_{-0.002} M_\odot$ [6]. Both panels are constructed from the Gogny and MDI parametrizations used in this work. The blue solid circle with error bars (panel a) is related to the constraint extracted from the GW170817 event [7]. Grey band: predictions from Skyrme parametrizations consistent with constraints from symmetric and asymmetric nuclear matter [29,78].

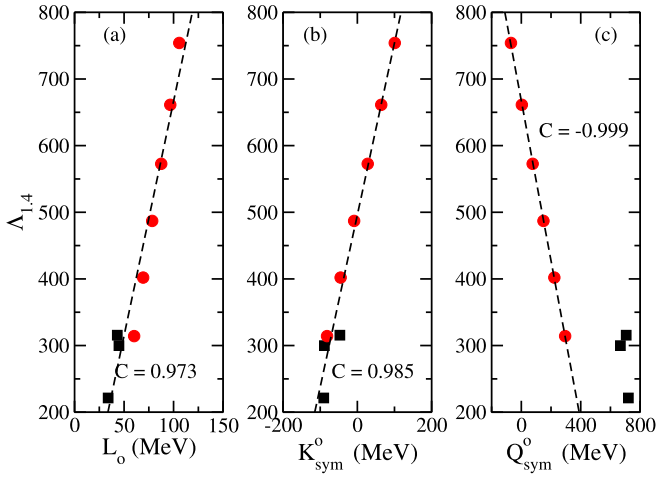

Fig. 3. Results from Gogny (black squares) and MDI (red circles) models for $\Lambda_{1.4}$ as a function of (a) symmetry energy slope, (b) symmetry energy curvature and (c) symmetry energy skewness, all of them at the saturation density. Dashed lines: fitting curves.

origin of the power not equal to 5 in the $\Lambda_{1.4} \times R_{1.4}$ relationship. Different a and b values are found for different relativistic and nonrelativistic models, as one can verify for instance in Refs. [9,23,24]. Such a relation has also been derived in Ref. [77] from a very general approach based on a parameterization of the speed of sound. The relation $\Lambda_{1.4} \times R_{1.4}$ is important, in particular, since there is a range for $\Lambda_{1.4}$ provided by the LVC, namely, $\Lambda_{1.4} = 190^{+390}_{-120}$. If we combine this range with our fitting expression $\Lambda_{1.4} = a R^b_{1.4}$, it is possible to extract a respective range of $R_{1.4}$ by inverting the expression as $R_{1.4} = (\Lambda_{1.4}/a)^{1/b}$. By applying the boundary values of $\Lambda_{1.4} = 70$ and $\Lambda_{1.4} = 580$, one can extract a range of 9.3 km $\leq R_{1.4} \leq$ 13.1 km for the radius of a canonical NS. This range is very similar to the one predicted in Ref. [37], namely, 9.0 km $\leq R_{1.4} \leq$ 13.6 km, where the authors confront the LVC data with their theoretical analysis.

In Fig. 2b we show the tidal deformabilities Λ_1 and Λ_2 of a binary NS system calculated with the Gogny and MDI parametrizations along with the contour line of 90% credible level (dashed blue curve) related to the GW170817 NS merger event [7]. To generate the curves, we vary the mass of one of the stars in the binary system, m_1, in the range $1.36 \leq m_1/M_\odot \leq 1.60$ [7,8]. The mass of the companion star, m_2, is related to m_1 through the so-called chirp mass $\mathcal{M}$, which is given by $\mathcal{M} = (m_1 m_2)^{3/5}/(m_1 + m_2)^{1/5}$. The GW170817 detection provides a chirp mass of $\mathcal{M} = 1.188^{+0.004}_{-0.002} M_\odot$ [6]. Hence, m_2 varies in the ranges $1.17 \leq m_2/M_\odot \leq 1.36$ [6,7]. From Fig. 2b we find a good agreement between the results obtained with the Gogny and MDI parametrizations used in this work and the LIGO/Virgo data. We also compare the present results with the values provided by the widely-known Skyrme model [29]. In that work, the authors calculated the tidal deformabilities for a set of Skyrme forces that are consistent with the constraints in symmetric and asymmetric nuclear matter discussed in Ref. [78]. We see that all the Gogny forces analyzed here lie inside the region defined by the Skyrme models, which is represented by the gray band in Fig. 2b. A similar kind of agreement is found for MDI with $x = 0$ and $x = 0.2$.

Another investigation performed in this work is the search for possible correlations between the tidal deformability $\Lambda_{1.4}$ and the bulk parameters of nuclear matter. Since $\Lambda_{1.4}$ is constrained by the LIGO/Virgo analysis of the GW170817 NS merger event, correlations between this quantity and a generic nuclear quantity $\mathcal{A}$ may help to establish boundaries on $\mathcal{A}$, and, consequently, to better constrain the microphysics related to the EoS of the hadronic model. This is the case for the nuclear matter bulk parameters [79–81]. In Figs. 3a and 3b, we display $\Lambda_{1.4}$ as a function of L_0 and $K^0_{\rm sym}$, namely, the symmetry energy slope and energy curvature (both at the saturation density) with the respective fitting curves applied to the considered Gogny and MDI parametrizations. In Fig. 3c we show how $\Lambda_{1.4}$ depends on the symmetry energy skewness at the saturation density, $Q^0_{\rm sym}$. Here, the fitting curve is obtained only for the MDI parametrizations, since we have not enough points related to the Gogny model. From the figure, we verify a strong correlation of $\Lambda_{1.4}$ with L_0 and $K^0_{\rm sym}$, as the fitted curves show a high correlation coefficient. The increasing of $\Lambda_{1.4}$ with L_0 was also verified in Ref. [38], in which the authors used a set of unified equations of state based on the Skyrme model. We find in Fig. 3c a high correlation of $\Lambda_{1.4}$ with $Q^0_{\rm sym}$ within the MDI model. However, although there are only few Gogny points, the results suggest that the trend for $\Lambda_{1.4}$ with $Q^0_{\rm sym}$ is different for Gogny and MDI models. Analyzing in addition the predictions of several Skyrme parametrizations (not shown) we have also observed that the correlation of $\Lambda_{1.4}$ with $Q^0_{\rm sym}$ is weak among different models. One can assign this larger deviation to the higher-order derivative of the symmetry energy, i.e., small variations on the symmetry energy are enough to cause larger variations on $Q^0_{\rm sym}$ (third derivative of the symmetry energy).

One can use the given correlations and the observational range for $\Lambda_{1.4}$ predicted in Ref. [7] to determine compatible ranges for L_0

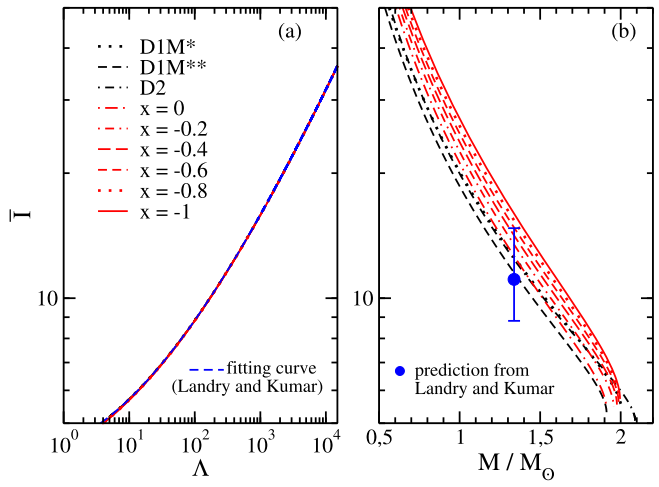

Fig. 4. Results from Gogny and MDI models for the dimensionless moment of inertia $\bar{I}$ as a function of (a) dimensionless tidal deformability, and (b) neutron star mass. Dashed blue curve: fitting curve obtained in Ref. [14]. Blue circle with error bars: predictions from Ref. [14] for $\bar{I}_\star$, namely, the dimensionless moment of inertia of the PSR J0737-3039 primary component pulsar.

and $K^0_{\rm sym}$. By applying this procedure we find that the dimensionless tidal deformability of the canonical neutron star obtained by the LIGO/Virgo collaboration, namely, $\Lambda_{1.4} = 190^{+390}_{-120}$, can be satisfactorily described by parametrizations presenting $15\,\text{MeV} \leq L_0 \leq 88\,\text{MeV}$ and $-165\,\text{MeV} \leq K^0_{\rm sym} \leq 33\,\text{MeV}$. As we have discussed before, interactions with slope parameter $L_0 \lesssim 40$ MeV seem to be unable to provide NSs of $M_{\rm max}$ of $2M_\odot$. This constraint, applied to Fig. 3a, points to a lower bound of $\Lambda_{1.4} \gtrsim 244$, which in turn implies a lower bound of -98 MeV for $K^0_{\rm sym}$.

We also remark that such constraints on the nuclear matter bulk parameters obtained from their relation with $\Lambda_{1.4}$ are an attempt to find a general trend for the values of these quantities. In that sense, they are model dependent and a more systematic study including other kind of hadronic models is needed in order to confirm or improve these numbers. Concerning the range for $K^0_{\rm sym}$, for instance, it is worth to mention that it is similar to the one suggested in Ref. [57], in which the authors proposed a metamodeling approach to treat the EoS for dense nuclear matter, namely, $K^0_{\rm sym} = -100 \pm 100$ MeV. Regarding the range of L_0, on the other hand, there are more stringent bounds found from combined analyses of astrophysical and nuclear data, see Ref. [56] for instance.

All of the Gogny and MDI parametrizations analyzed in this work show similar bulk properties in symmetric nuclear matter, with saturation density $\rho_0 \sim 0.16$ fm^{-3}, energy per particle $E_0 \sim -16$ MeV, effective mass $m^*_0/m \sim 0.7$, incompressibility K_0 between 209 and 225 MeV, and skewness Q_0 between -460 and -427 MeV. In the isovector sector, we find a similar situation for the symmetry energy $E^0_{\rm sym}$ at saturation, which shows a limited variation ($E^0_{\rm sym} = 28.5 - 31$ MeV) in the considered parametrizations. Therefore, this fact can be the origin of the very small interference of these bulk parameters in possible correlations arising from $\Lambda_{1.4}$ as a function of L_0, $K^0_{\rm sym}$ and $Q^0_{\rm sym}$.

Finally, we show in Fig. 4 the dimensionless moment of inertia, $\bar{I} \equiv I/M^3$, calculated from the Gogny and MDI models. We obtain this quantity by solving the Hartle's slow rotation equation given in Refs. [11,14,82], namely, a differential equation for one of the metric decomposition functions [11], $\omega(r)$, coupled to the TOV equations. The moment of inertia is given in terms of $\omega_R \equiv \omega(R)$ as $I = R^3(1-\omega_R)/2$, where ω_R is the frame-dragging function $\omega(r)$ [14] evaluated at the surface of the star in which $r = R$. In Fig. 4a, one can verify that all used Gogny and MDI interactions are indistinguishable in the plot of $\bar{I}$ as a function of Λ. Such a feature is claimed to be universal and is known as the I-Love relation. In Refs. [10,11], using a set of 10 different EoSs, the authors showed that such a relation is independent of the neutron star (or quark star) structure for slowly-rotating stars. In Ref. [14], the same result was obtained for a set of 53 Skyrme and relativistic mean-field parametrizations. Here, we show that the same feature remains for the Gogny and MDI finite-range nuclear interactions, thereby confirming the universality of the I-Love relation also with this class of models. In Fig. 4a we display by a dashed line the fitting curve determined in Ref. [14]. We see that the Gogny and MDI models are compatible with this fitting.

In Ref. [14], the authors also determined a range for $\bar{I}$ related to the PSR J0737-3039 primary component pulsar (a pulsar of mass $M_\star = 1.338 M_\odot$), namely, $\bar{I}_\star \equiv \bar{I}(M_\star) = 11.10^{+3.68}_{-2.28}$. Measurements regarding this slowly rotating pulsar are expected to determine its moment of inertia in the next few years with hitherto unachieved accuracy ($\sim$10%). Such a range of Ref. [14] was calculated, using the candidate Skyrme and relativistic mean-field EoSs, in two steps. First, the authors of [14] verified a relation between $\Lambda_\star$ and $\Lambda_{1.4}$, called as the binary-Love relation. Here, $\Lambda_\star$ is the dimensionless tidal deformability related to the star of mass $M_\star$. Then, they used a suitable fitting for $\Lambda_\star$ as a function of $\Lambda_{1.4}$ along with the I-Love relation fitting curve presented in Fig. 4a to establish $\bar{I}_\star$ as a function of $\Lambda_\star$. Finally, the observational range $\Lambda_{1.4} = 190^{+390}_{-120}$ obtained by the LIGO/Virgo collaboration was used to determine a range for $\Lambda_\star$, and consequently, the limits of $\bar{I}_\star = 11.10^{+3.68}_{-2.28}$. As one can see in Fig. 4b, the Gogny parametrizations used present $\bar{I}_\star$ inside the predicted range. For the MDI interactions, those in which $x > -0.6$ are also in agreement with the limits. The fact that the Gogny and MDI forces that fulfill the LVC observational bounds $\Lambda_{1.4} = 190^{+390}_{-120}$ also agree with the range of Ref. [14] for $\bar{I}$, corroborates with another type of hadronic models, the limits for the moment of inertia of pulsar A of PSR J0737-3039 established by Landry and Kumar [14].

4. Summary and concluding remarks

We have studied the predictions of the EoS of stellar matter from finite-range effective interactions of the Gogny and MDI types for describing NS properties related with the information extracted from the GW170817 detection of gravitational waves by the LIGO/Virgo collaboration. The tidal deformability $\Lambda_{1.4}$ predicted by the Gogny and MDI interactions for a $1.4M_\odot$ NS agrees with the corresponding data supplied by LIGO/Virgo, except for the MDI interactions with $x = -0.8$ and $x = -1$, which have the stiffest symmetry energies of the considered models. From the dependence of $\Lambda_{1.4}$ with the NS radius $R_{1.4}$ obtained with the Gogny and MDI interactions, the LVC observational value $\Lambda_{1.4} = 190^{+390}_{-120}$ allows one to constrain the radius of a canonical NS in the range of $9.3\,\text{km} \leq R_{1.4} \leq 13.1\,\text{km}$. We have also calculated the tidal deformabilities of the two NSs in the binary system assuming the chirp mass that was measured in the GW170817 event. The results lie within the 90% confidence region extracted from the LIGO/Virgo data for most of the analyzed parametrizations.

We have seen that the isoscalar properties and the value of the symmetry energy at saturation of the underlying Gogny and MDI interactions used to build the stellar EoS have little impact on the tidal deformability $\Lambda_{1.4}$ computed with these models, while $\Lambda_{1.4}$ shows a clear dependence, roughly linear, with the isovector properties of the interaction, such as the slope (L_0), curvature ($K^0_{\rm sym}$) and skewness ($Q^0_{\rm sym}$) of the symmetry energy. We find that the LIGO/Virgo determination of $\Lambda_{1.4}$ can be reproduced by the effective interactions characterized by $15\,\text{MeV} \leq L_0 \leq 88\,\text{MeV}$ and $-165\,\text{MeV} \leq K^0_{\rm sym} \leq 33\,\text{MeV}$. In particular, the L_0 range is in harmony with other estimates of the slope of the symmetry energy

derived from nuclear observables such as the neutron skin thickness, giant resonances, heavy-ion reactions, or the systematics of nuclear masses (see, for instance, [83] and references therein). Finally, we have analyzed the moment of inertia of a NS as a function of the tidal deformability. We have shown that the so-called I-Love relation [10,11], which is expected to be universal, is, indeed, also satisfied by the Gogny and MDI interactions. In addition, we obtain that the prediction of Landry and Kumar [14] of a dimensionless moment of inertia $\bar{I}_\star = 11.10^{+3.68}_{-2.28}$ for PSR J0737-3039 is supported by the Gogny and MDI models that, at the same time, are consistent with the LIGO/Virgo determination of $\Lambda_{1.4}$.

Acknowledgements

This work is a part of the project INCT-FNA Proc. No. 464898/2014-5, partially supported by Conselho Nacional de Desenvolvimento Científico e Tecnológico (CNPq) under grants 310242/2017-7 and 406958/2018-1 (O.L.), and 433369/2018-3 (M.D.), and by Fundação de Amparo à Pesquisa do Estado de São Paulo (FAPESP) under the thematic projects 2013/26258-4 (O.L.) and 2017/05660-0 (O.L., M.D.). C.G, M.C. and X.V. acknowledge support from Grant FIS2017-87534-P from MINECO and FEDER, and Project MDM-2014-0369 of ICCUB (Unidad de Excelencia María de Maeztu) from MINECO. C.G. also acknowledges Grant BES-2015-074210 from MINECO.

References

[1] N.K. Glendenning, J. Schaffner-Bielich, Phys. Rev. C 60 (1999) 025803.
[2] C.B. Haakonsen, M. Turner, N.A. Tacik, R.E. Rutledge, Astrophys. J. 749 (2012) 52.
[3] A.W. Steiner, J.M. Lattimer, E.F. Brown, Astrophys. J. Lett. 765 (2013) L5.
[4] J.M. Lattimer, A.W. Steiner, Astrophys. J. 784 (2014) 123.
[5] F. Özel, P. Freire, Annu. Rev. Astron. Astrophys. 54 (2016) 401.
[6] B.P. Abbott, et al., LIGO Scientific Collaboration Virgo Collaboration, Phys. Rev. Lett. 119 (2017) 161101.
[7] B.P. Abbott, et al., LIGO Scientific Collaboration Virgo Collaboration, Phys. Rev. Lett. 121 (2018) 161101.
[8] B.P. Abbott, et al., LIGO Scientific Collaboration Virgo Collaboration, Phys. Rev. X 9 (2019) 011001.
[9] T. Malik, N. Alam, M. Fortin, C. Providência, B.K. Agrawal, T.K. Jha, Bharat Kumar, S.K. Patra, Phys. Rev. C 98 (2018) 035804.
[10] K. Yagi, N. Yunes, Science 341 (2013) 365.
[11] K. Yagi, N. Yunes, Phys. Rev. D 88 (2013) 023009.
[12] K. Yagi, N. Yunes, Class. Quantum Gravity 34 (2016) 015006.
[13] C. Pankow, K. Chatziioannou, Eve A. Chase, T.B. Littenberg, M. Evans, J. McIver, N.J. Cornish, Carl-Johan Haster, J. Kanner, V. Raymond, S. Vitale, A. Zimmerman, Phys. Rev. D 98 (2018) 084016.
[14] P. Landry, B. Kumar, Astrophys. J. Lett. 868 (2018) L22.
[15] P.B. Demorest, T. Pennucci, S.M. Ransom, M.S.E. Roberts, J.W.T. Hessels, Nature 467 (2010) 1081.
[16] E. Fonseca, T.T. Pennucci, J.A. Ellis, I.H. Stairs, D.J. Nice, et al., Astrophys. J. 832 (2016) 167.
[17] J. Antoniadis, P.C.C. Freire, N. Wex, et al., Science 340 (2013) 448.
[18] M. Oertel, H. Hempel, T. Klähn, S. Typel, Rev. Mod. Phys. 89 (2017) 015007.
[19] A. Li, G.V. Ramos, I. Vidana, Eur. Phys. J. A 50 (2014) 2.
[20] L.C. Stein, K. Yagi, N. Yunes, Astrophys. J. 788 (2014) 15.
[21] J. Nättilä, A.W. Steiner, J.J.E. Kajava, V.F. Suleimanov, J. Poutanen, Astron. Astrophys. 591 (2016) A25.
[22] S. De, D. Finstad, J.M. Lattimer, D.A. Brown, E. Berger, C.M. Biwer, Phys. Rev. Lett. 121 (2018) 091102.
[23] E. Annala, T. Gorda, A. Kurkela, A. Vuorinen, Phys. Rev. Lett. 120 (2018) 172703.
[24] F.J. Fattoyev, J. Piekarewicz, C.J. Horowitz, Phys. Rev. Lett. 120 (2018) 172702.
[25] E.R. Most, L.R. Weih, L. Rezzolla, J. Schaffner-Bielich, Phys. Rev. Lett. 120 (2018) 261103.
[26] N.K. Glendenning, Astrophys. J. 293 (1985) 470.
[27] S. Gandolfi, J. Carlson, S. Reddy, Phys. Rev. C 85 (2012) 032801.
[28] V. Paschalidis, K. Yagi, D. Alvarez-Castillo, D.B. Blaschke, A. Sedrakian, Phys. Rev. D 97 (2018) 084038.
[29] O. Lourenço, M. Dutra, C.H. Lenzi, S.K. Biswal, M. Bhuyan, D.P. Menezes, Eur. Phys. J. A 56 (2020) 32.
[30] K. Hebeler, S.K. Bogner, R.J. Furnstahl, A. Nogga, A. Schwenk, Phys. Rev. C 83 (2011) 031301.
[31] N. Kaiser, Eur. Phys. J. A 48 (2012) 135.
[32] M. Buballa, Phys. Rep. 407 (2005) 205.
[33] S. Benic, D. Blaschke, D.E. Alvarez-Castillo, T. Fischer, S. Typel, Astron. Astrophys. 577 (2015) A40.
[34] K. Fukushima, T. Hatsuda, Rep. Prog. Phys. 74 (2011) 014001.
[35] M.G. Alford, K. Rajagopal, F. Wilczek, Phys. Lett. B 422 (1998) 247.
[36] I.F. Ranea-Sandoval, S. Han, M.G. Orsaria, G.A. Contrera, F. Weber, M.G. Alford, Phys. Rev. C 93 (2016) 045812.
[37] I. Tews, J. Margueron, S. Reddy, Phys. Rev. C 98 (2018) 045804.
[38] L. Perot, N. Chamel, A. Sourie, Phys. Rev. C 100 (2019) 035801.
[39] C.Y. Tsang, M.B. Tsang, P. Danielewicz, F.J. Fattoyev, W.G. Lynch, Phys. Lett. B 796 (2019) 1.
[40] O. Lourenço, M. Dutra, C.H. Lenzi, M. Bhuyan, S.K. Biswal, B.M. Santos, Astrophys. J. 882 (2019) 67.
[41] C. Gonzalez-Boquera, M. Centelles, X. Viñas, A. Rios, Phys. Rev. C 96 (2017) 065806.
[42] C. Gonzalez-Boquera, M. Centelles, X. Viñas, L.M. Robledo, Phys. Lett. B 779 (2018) 195.
[43] C.B. Das, S. Das Gupta, C. Gale, B.-A. Li, Phys. Rev. C 67 (2003) 034611.
[44] J. Xu, L.-W. Chen, B.-A. Li, H.-R. Ma, Astrophys. J. 697 (2009) 1549.
[45] J.-F. Berger, M. Girod, D. Gogny, Comput. Phys. Commun. 63 (1991) 365.
[46] CEA web page www-phynu.cea.fr.
[47] F. Chappert, M. Girod, S. Hilaire, Phys. Lett. B 668 (2008) 420.
[48] S. Goriely, S. Hilaire, M. Girod, S. Péru, Phys. Rev. Lett. 102 (2009) 242501.
[49] B. Friedman, V. Pandharipande, Nucl. Phys. A 361 (1981) 502.
[50] F. Chappert, N. Pillet, M. Girod, J.-F. Berger, Phys. Rev. 91 (2015) 034312.
[51] X. Viñas, C. Gonzalez-Boquera, M. Centelles, L.M. Robledo, C. Mondal, Nucl. Theory 37 (2018) 68.
[52] B.-A. Li, L.W. Chen, C.M. Ko, Phys. Rep. 464 (2008) 113.
[53] P.G. Krastev, B.-A. Li, J. Phys. G 46 (2019) 074001.
[54] B.-A. Li, X. Han, Phys. Lett. B 727 (2013) 276.
[55] M. Dutra, O. Lourenço, S.S. Avancini, B.V. Carlson, A. Delfino, D.P. Menezes, C. Providência, S. Typel, J.R. Stone, Phys. Rev. C 90 (2014) 055203.
[56] J.M. Lattimer, Y. Lim, Astrophys. J. 771 (2013) 51.
[57] J. Margueron, R.H. Casali, F. Gulminelli, Phys. Rev. C 97 (2018) 025805.
[58] R.C. Tolman, Phys. Rev. 55 (1939) 364.
[59] J.R. Oppenheimer, G.M. Volkoff, Phys. Rev. 55 (1939) 374.
[60] G. Baym, C. Pethick, P. Sutherland, Astrophys. J. 170 (1971) 299.
[61] B. Link, R.I. Epstein, J.M. Lattimer, Phys. Rev. Lett. 83 (1999) 3362.
[62] J. Carriere, C. Horowitz, J. Piekarewicz, Astrophys. J. 593 (2003) 463.
[63] J. Piekarewicz, F.J. Fattoyev, Phys. Rev. C 99 (2019) 045802.
[64] S. Kubis, Phys. Rev. C 70 (2004) 065804.
[65] C. Gonzalez-Boquera, M. Centelles, X. Viñas, T.R. Routray, Phys. Rev. C 100 (2019) 015806.
[66] M. Fortin, C. Providência, A.R. Raduta, F. Gulminelli, J.L. Zdunik, P. Haensel, M. Bejger, Phys. Rev. C 94 (2016) 035804.
[67] T. Hinderer, B.D. Lackey, Ryan N. Lang, J.S. Read, Phys. Rev. D 81 (2010) 123016.
[68] J.S. Read, L. Baiotti, J.D.E. Creighton, J.L. Friedman, B. Giacomazzo, K. Kyutoku, C. Markakis, L. Rezzolla, M. Shibata, K. Taniguchi, Phys. Rev. D 88 (2013) 044042.
[69] Walter Del Pozzo, Tjonnie G.F. Li, Michalis Agathos, Chris Van Den Broeck, Phys. Rev. Lett. 111 (2013) 071101.
[70] S. Postnikov, M. Prakash, J.M. Lattimer, Phys. Rev. D 82 (2010) 024016.
[71] T. Hinderer, Astrophys. J. 677 (2008) 1216.
[72] T. Damour, A. Nagar, Phys. Rev. D 81 (2010) 084016.
[73] Binnington Taylor, Eric Poisson, Phys. Rev. D 80 (2009) 084018.
[74] A.W. Steiner, J.M. Lattimer, E.F. Brown, Astrophys. J. 722 (2010) 33.
[75] H.T. Cromartie, et al., Nat. Astron. Lett. 4 (2020) 72, arXiv:1904.06759.
[76] N. Alam, B.K. Agrawal, M. Fortin, H. Pais, C. Providência, Ad.R. Raduta, A. Sulaksono, Phys. Rev. C 94 (2016) 052801(R).
[77] I. Tews, J. Margueron, S. Reddy, Eur. Phys. J. A 55 (2019) 97.
[78] M. Dutra, O. Lourenço, J.S. Sá Martins, A. Delfino, J.R. Stone, P.D. Stevenson, Phys. Rev. C 85 (2012) 035201.
[79] B.M. Santos, M. Dutra, O. Lourenço, A. Delfino, Phys. Rev. C 90 (2014) 035203.
[80] J. Piekarewicz, M. Centelles, Phys. Rev. C 79 (2009) 054311.
[81] E. Khan, J. Margueron, I. Vidaña, Phys. Rev. Lett. 109 (2012) 092501.
[82] J.B. Hartle, Astrophys. J. 150 (1967) 1005.
[83] X. Viñas, M. Centelles, X. Roca-Maza, M. Warda, Eur. Phys. J. A 50 (2014) 27.